

2HDM(II) radiative corrections in leptonic tau decays

Maria Krawczyk¹ and David Temes²

1. *Institute of Theoretical Physics, University of Warsaw, ul. Hoża 69
Warsaw, 00-681, Poland*

2. *Laboratoire de Physique Théorique LAPTH
Ch. de Bellevue, B.P 110, F-74941, Annecy-le-Vieux, Cedex, France.*³

Abstract

The one-loop contributions to the branching ratios for leptonic τ decays are calculated in the CP conserving 2HDM(II). We found that these one-loop contributions, involving both neutral and charged Higgs bosons, dominate over the tree level H^\pm exchange, the latter one being totally negligible for the decay into e . The analysis is focused on large $\tan\beta$ enhanced contributions to the considered branching ratios and we derive a simple analytical expression for the one-loop contribution in this case. The leptonic branching ratios of τ have a large potential on constraining parameters of the model, being complementary to direct searches through Higgsstrahlung processes for $h(H)$. In this work, we provide upper limits on Yukawa couplings for both light h and light A scenarios and we derive new lower limit on mass of M_{H^\pm} as a function of $\tan\beta$, which differs significantly from what was considered as standard constraint based on the tree H^\pm exchange only. Interestingly we obtain also an upper limit on M_{H^\pm} . For a SM-like h scenario, with heavy and degenerate additional Higgs bosons, one-loop corrections disappear.

³URA 14-36 du CNRS, associée à l'Université de Savoie

1 Introduction

The mechanism of electroweak symmetry breaking is the most important unknown block in the description of elementary particle physics. The Standard Model (SM) incorporates the Higgs mechanism that breaks the electroweak symmetry spontaneously through a neutral scalar field with non-zero vacuum expectation value. In the minimal version of this mechanism one scalar $SU(2)_L$ doublet is required, providing one physical particle: the Higgs boson. The search of this particle is one of the main aims of high energy physics and current searches at LEP exclude SM Higgs bosons with masses below 114.1 GeV at 95% C.L. [1]. In this context, valuable information about the Higgs mass will come from analysis of precise measurements of electroweak observables. The result of these indirect searches gives an upper bound on the Higgs mass $M_{H_{SM}} < 219$ GeV at 95% C.L. [1], that is of great importance for future searches.

Models with Two Higgs Doublets (2HDM) are the minimal extensions of the SM Higgs sector describing all high energy experimental data and providing new and rich phenomenology. These models can also be interpreted as effective theories describing low-energy physics in models with beyond the SM physics at higher scale. This is the case of the Minimal Supersymmetric Standard Model (MSSM) with heavy supersymmetric particles, that gives a 2HDM at low energy. A CP-conserving 2HDM contains 5 physical Higgs bosons, two neutral scalars, h and H , one pseudoscalar A , and two charged Higgs bosons, H^\pm (see e.g. [2]). The analysis of LEP direct searches for these Higgs bosons is more complicated than in the SM due to the number of free parameters involved and, in particular, the existence of a light Higgs boson can not be excluded [1]. However, LEP data highly constrains the 2HDM parameter space excluding, for example, neutral Higgs bosons with masses below 40 GeV in the large $\tan\beta$ regime [3].

In this context, indirect searches for 2HDM effects in electroweak observables will provide important information about the values of masses and mixing angles in the Higgs sector. For example, concerning the charged Higgs, a lower bound $M_{H^\pm} > 490$ GeV can be set using indirect effects on $b \rightarrow s\gamma$ [4], to compare with $M_{H^\pm} > 75.5$ GeV coming from direct LEP searches [5]. In order to explore the whole parameter space, global fits using different electroweak observables ρ , R_b and $b \rightarrow \gamma$ [6, 7] (and also $(g-2)_\mu$ in [7]), have been made, constraining large regions of the parameter space and therefore giving valuable information for future searches.

In this work, the study of one-loop 2HDM effects in leptonic τ decays is performed without any assumption on the Higgs spectrum, generalising the result from [8]. It will be seen that this radiative effects are larger than the 2HDM tree-level effects in the relevant regions of parameter space and experimental data will be used to derive new constraints in Higgs masses and mixing angles.

The paper is organised as follows. In Sect. 2 a short description on the

2HDM properties, together with experimental searches on Higgs bosons is performed. In Sect. 3 and 4 the leptonic τ decay data is compared with the SM prediction and the 2HDM contributions to these decays are parameterised. The one-loop 2HDM(II) effects are computed in Sect. 5 while their numerical analysis is performed in Sec. 6. Finally, in Sect. 7 we derived the constraints on the 2HDM(II) parameters coming from leptonic τ decay data analysis and our conclusions are summarised in Sect. 8.

2 CP conserving 2HDM of type II

2.1 General properties

The Two-Higgs-Doublet Model is the simplest extension of the Standard Model with one extra scalar doublet. It contains three neutral and two charged Higgs bosons. Here we consider a simple CP conserving version with a soft Z_2 -violation, assuming the Yukawa interactions according to the Model II, as in MSSM. In this model one of the Higgs scalar doublet couples to the up-components of isodoublets while the second one to the down-components. In this case there are 7 parameters describing the Higgs Lagrangian: four masses for h, H, A and H^\pm , two mixing angles α and β (used in form $\sin(\beta - \alpha)$ and $\tan \beta = v_2/v_1$), and the ν -parameter, related to the soft- Z_2 violating mass term in the Lagrangian. This ν -parameter describes the Higgs selfcouplings if they are expressed in terms of masses, we stress that none of these couplings are involved in this analysis explicitly.

An attractive possibility to consider is the one with the neutral Higgs boson h similar to the SM one, while the others are much heavier. This scenario can be realised in two ways, depending on the value of the ν -parameter. For large ν the additional Higgs boson masses can be very large and there is a *decoupling* of these heavy bosons from known particles, i.e. effects of these additional Higgs bosons disappear if their masses are degenerate and tend to infinity, eg. in the $\gamma\gamma h$ coupling. At small ν , the masses of such additional Higgs bosons are bounded from above by the unitarity constraints on Higgs selfcouplings [9]. However, these additional Higgs bosons can be heavy enough, with masses say 600 GeV, to avoid observation even at next generation of colliders. In this scenario, some relevant effects can appear for the lightest Higgs boson [10–13].

Another interesting scenarios that will be intensively studied in this work are the ones with h or A lighter than the SM bound on the Higgs mass, 114 GeV. In particular the light A scenario is specially interesting for the description of $(g-2)_\mu$ data [14–16]. These scenarios are possible within a 2HDM(II), which allows for low production rates for very light Higgs particles, as discussed below.

The couplings to fermions and to gauge bosons, relative to the corresponding ones in the SM, $\chi_j^i = g_j^i/g_j^{SM}$, are presented in Table 1. Note

that

$$(\chi_V^h)^2 + (\chi_V^H)^2 + (\chi_V^A)^2 = 1,$$

and similarly for couplings to fermions [10].

Table 1: *Relative couplings*, $\chi_j^i = g_j^i/g_j^{SM}$

	h	H	A
χ_V	$\sin(\beta - \alpha)$	$\cos(\beta - \alpha)$	0
χ_u	$\frac{\cos \alpha}{\sin \beta} = \chi_V^h + \cot \beta \chi_V^H$	$\frac{\sin \alpha}{\sin \beta} = \chi_V^H - \cot \beta \chi_V^h$	$-i \cot \beta$
χ_d	$-\frac{\sin \alpha}{\cos \beta} = \chi_V^h - \tan \beta \chi_V^H$	$\frac{\cos \alpha}{\cos \beta} = \chi_V^H + \tan \beta \chi_V^h$	$-i \tan \beta$
χ_{VH^+}	$\cos(\beta - \alpha)$	$\sin(\beta - \alpha)$	0

Note, that for large $\tan \beta$ couplings to charged leptons are enhanced. Note also, the for each neutral Higgs boson we have

$$(\chi_u^i + \chi_d^i)\chi_V^i = 1 + \chi_u^i \chi_d^i.$$

The $W^\pm H^\mp \phi^0$ couplings, with $\phi^0 = h, H, A$, will be of interest in this work. In the last row of Table 1 the dependence of the ratios of the $W^\pm H^\mp \phi^0$ couplings to the Standard Model Higgs coupling to gauge boson, $\chi_{VH^+}^i = g_{W^\pm H^\mp}^i/g_V^{SM}$, on the α and β angles is showed.

It is important to notice the complementarity in the $\sin(\beta - \alpha)$ dependence between χ_V^i on one hand and $\chi_{VH^+}^i$ and χ_d^i at large $\tan \beta$ on the other.

2.2 Experimental constraints on 2HDM

The most important constraints on the 2HDM(II) parameter space come from LEP direct searches of Higgs bosons. Concerning light neutral Higgs bosons production, there are three main processes within the energy range covered by LEP, namely, the Higgsstrahlung, $e^+e^- \rightarrow Z^* \rightarrow Zh$, the associated production, $e^+e^- \rightarrow Z^* \rightarrow hA$, and the Yukawa processes, $e^+e^- \rightarrow f\bar{f} \rightarrow f\bar{f}h(A)$. The two first processes are highly complementary, due to their dependence on $\sin^2(\beta - \alpha)$,

$$\sigma(e^+e^- \rightarrow Z^* \rightarrow Zh) = \sin^2(\beta - \alpha)\sigma_{SM}(e^+e^- \rightarrow Z^* \rightarrow ZH_{SM})$$

$$\sigma(e^+e^- \rightarrow Z^* \rightarrow hA) = \cos^2(\beta - \alpha)\sigma_{SM}(e^+e^- \rightarrow Z^* \rightarrow ZH_{SM})\bar{\lambda} \quad (1)$$

$$\sigma(e^+e^- \rightarrow Z^* \rightarrow f\bar{f}h) = (\chi_d^h)^2\sigma_{SM}(e^+e^- \rightarrow Z^* \rightarrow f\bar{f}H_{SM}) \quad (2)$$

$$\sigma(e^+e^- \rightarrow Z^* \rightarrow f\bar{f}A) = (\chi_d^A)^2\sigma_{SM}(e^+e^- \rightarrow Z^* \rightarrow f\bar{f}H_{SM}), \quad (3)$$

where $\bar{\lambda} = \lambda_{Ah}^{3/2}/[\lambda_{Zh}^{1/2}(12M_Z^2/s + \lambda_{Zh})]$ being $\lambda_{ij} = (1 - m_i^2/s + m_j^2)^2 - 4m_i^2m_j^2/s^2$ the two-particle phase-space factor.

The search for a light h through the Higgsstrahlung process has been performed assuming that the light Higgs boson decays into hadronic states [17].

The results of this analysis set an upper limit on the product of the cross section and the branching ratio as a function of the light Higgs mass and they can be translated into an upper limit on $\sin^2(\beta - \alpha)$ as a function of M_h . This main result is drawn in Fig. 1 (left) [17]. Therefore, the results of this analysis are compatible with a light h scenario (with mass below 114 GeV) if $\sin^2(\beta - \alpha)$ is small enough.

Also upper limits on the cross section of the associated hA production process have been derived assuming 100% decays into hadrons [18]. These results can be translated into forbidden regions in the 2HDM(II) parameter space that, in particular, highly constrain a scenario with both h and A light. In Fig. 1 (right) the excluded $(M_h - M_A)$ regions have been plotted [18]. A particular point is excluded if it is excluded for $0.4 \leq \tan\beta \leq 40$ (darker grey region), $0.4 \leq \tan\beta \leq 1$ (lighter grey region), and $1 \leq \tan\beta \leq 40$ (hatched region) for all values $\alpha = \pm\pi/2, \pm\pi/4, 0$. It is noticeable that a scenario with light h (or A) is not excluded if M_A (or M_h) is large enough. In particular, if $\sin^2(\beta - \alpha) = 0$, LEP is sensitive to this associated production if $M_h + M_A \leq 130$ GeV.

Finally, the search for a light Higgs boson has been performed through the analysis of Yukawa processes and Higgs decays into τ , if $2m_\tau < M_h, M_A < 2m_b$, or into b -quarks, if $M_h, M_A > 2m_b$ [3]. One of the results of this analysis is that $M_{h,A} \leq 40$ GeV are excluded for high $\tan\beta$ ($\tan\beta \geq 60$). We will discuss existing constraints together with new ones coming from our analysis in Sect.7.

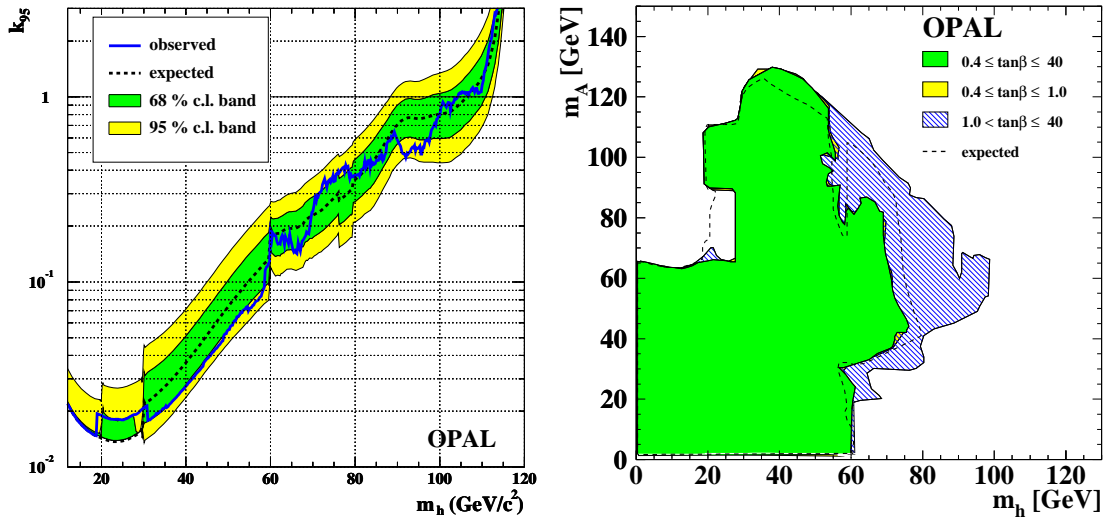


Figure 1: *Left: Upper limit on $\sin^2(\beta - \alpha)$ as a function of M_h [17]. Right: Excluded $(M_h - M_A)$ regions in different ranges of $\tan\beta$ for all $\alpha = \pm\pi/2, \pm\pi/4, 0$ [18].*

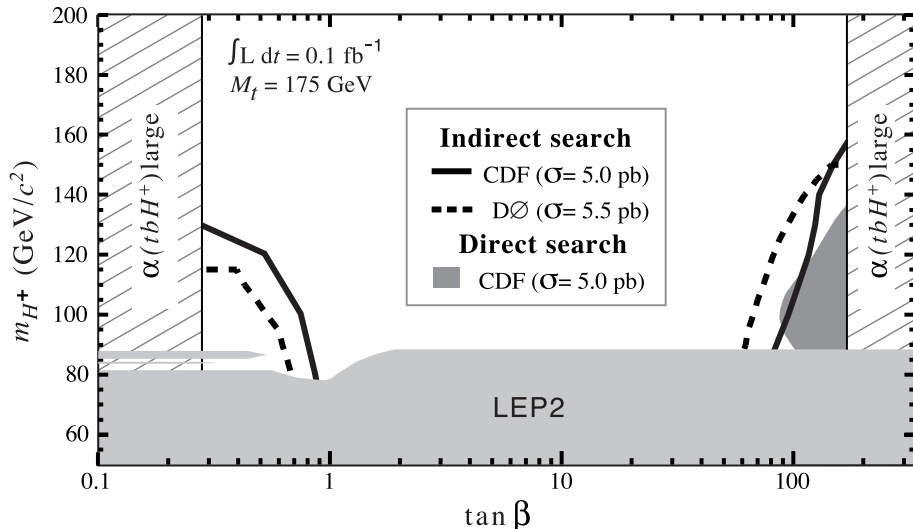


Figure 2: Constraints on charged Higgs boson mass [1].

Concerning the charged Higgs boson, direct searches at LEP through the process $e^+e^- \rightarrow H^+H^-$ have been performed assuming $BR(H^- \rightarrow q\bar{q}) + BR(H^- \rightarrow \tau\nu_\tau) = 1$, setting the lower bound $M_{H^\pm} \geq 75.5$ GeV at 95% CL [5]. Tevatron data set limits on mass of the charged Higgs boson as a function on $\tan\beta$, they are presented together with LEP results on Fig. 2.

Much stronger constraints on M_{H^\pm} come from indirect charged Higgs boson effects on $b \rightarrow s\gamma$ processes, if interpreted in a 2HDM(II) this leads to a lower mass limit of 490 GeV at 95% for $\tan\beta > 2$ [4]⁴.

In this context, important information on the available 2HDM(II) parameter space is expected from indirect searches on precision observables. In particular, from the Upsilon decay and $g - 2$ data, see eg. [16]. Also global fits have been performed, combining the results coming from the different electroweak observables ρ , R_b and $b \rightarrow \gamma$ [6, 7] (and also $(g - 2)_\mu$ in [7]), constraining large regions of the parameter space. Here, indirect searches of 2HDM(II) will be performed using leptonic τ decays data and the results will be compared with direct searches analysis coming from LEP and some low energy experiments. The implementation of leptonic τ decay data in global fits will be performed elsewhere.

⁴Recent analysis on $B \rightarrow X_s\gamma$ predicts larger theoretical errors in the SM prediction and therefore a more conservative lower bound $M_{H^\pm} \geq 200$ GeV [19].

3 Leptonic τ decays: data versus SM predictions

We consider the partial decay widths and branching ratios for the two leptonic decay channels of the τ -lepton:

$$\tau \rightarrow e\bar{\nu}_e\nu_\tau \text{ and } \tau \rightarrow \mu\bar{\nu}_\mu\nu_\tau. \quad (4)$$

We will denote the corresponding quantities using superscript l , $l = e$ and μ , for example for the branching ratio we use $Br^l = Br(\tau \rightarrow l\bar{\nu}_l\nu_\tau)$.

The '04 world averaged data for the leptonic τ decay modes and τ lifetime are [1]

$$Br^e|_{exp} = (17.84 \pm 0.06)\%, \quad Br^\mu|_{exp} = (17.37 \pm 0.06)\% \quad (5)$$

$$\tau_\tau = (290.6 \pm 1.1) \times 10^{-15} s. \quad (6)$$

Note that the relative errors of the above measured quantities are of the 0.34-0.38 %, the biggest being for the lifetime.

The SM prediction for these branching ratios can be defined as the ratios of the SM predicted decay widths to the total width as measured in the lifetime experiments, namely $Br^l|_{SM} = \Gamma^l|_{SM}/\Gamma_{exp}^{tot} = \Gamma^l|_{SM}\tau_\tau$. Therefore, one can parametrise a possible beyond the SM contribution by a quantity Δ^l , defined as

$$Br^l = Br^l|_{SM}(1 + \Delta^l). \quad (7)$$

In the lowest order of SM the leptonic decay width of the τ is due to the tree level W exchange, see Fig. 3 (left). Including the W-propagator effect and QED radiative corrections, the following results for the branching ratios in the SM are obtained (see also Sect. 4):

$$Br^e|_{SM} = (17.80 \pm 0.07)\%, \quad Br^\mu|_{SM} = (17.32 \pm 0.07)\%. \quad (8)$$

Together with the experimental data this leads to the following estimations for the possible beyond SM contributions to the considered branching ratios,

$$\Delta^e = (0.20 \pm 0.51)\%, \quad \Delta^\mu = (0.26 \pm 0.52)\%. \quad (9)$$

Using them we derive the 95% C.L. bounds on Δ^l , for the electron and muon decay mode, respectively:

$$(-0.80 \leq \Delta^e \leq 1.21)\%, \quad (-0.76 \leq \Delta^\mu \leq 1.27)\%. \quad (10)$$

One can see that the negative contributions are constrained more strongly than the positive ones.

4 Leptonic τ decays in 2HDM

In the SM the leptonic τ decay, $\tau \rightarrow l\bar{\nu}_l\nu_\tau$, proceeds at tree-level via the W^\pm exchange. The formula below describes this contribution in the Fermi approximation, with leading order corrections to the W propagator, and dominant QED one-loop contributions,

$$\Gamma^l|_{SM} = \Gamma_{tree}^{W^\pm} = \frac{G_F^2 m_\tau^5}{192\pi^3} f\left(\frac{m_l^2}{m_\tau^2}\right) \left(1 + \frac{3m_\tau^2}{5m_W^2} - 2\frac{m_l^2}{m_W^2}\right) \times \left(1 + \frac{\alpha(m_\tau)}{2\pi} \left(\frac{25}{4} - \pi^2\right)\right), \quad (11)$$

$$f(x) = 1 - 8x + 8x^3 - x^4 - 12x^2 \ln x. \quad (12)$$

We will denote the SM contribution in short as Γ_0^l , skipping here and below the superscript l if not necessary.

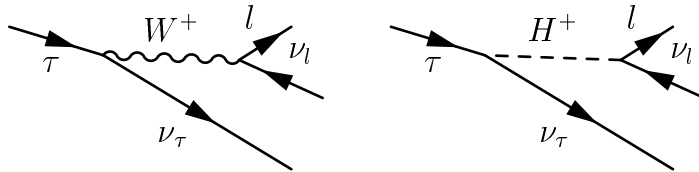


Figure 3: Tree-level contributions to the τ leptonic decays. The W^\pm exchange in the SM (on the left) and the H^\pm exchange in 2HDM (on the right).

In a 2HDM there is in addition a tree contribution due to the tree-level exchange of the charged Higgs boson, Fig. 3 (right). This new contribution is given by

$$\Gamma_{tree}^{H^\pm} = \Gamma_0 \left[\frac{m_\tau^2 m_l^2 \tan^4 \beta}{4M_{H^\pm}^4} - 2\frac{m_l^2 \tan^2 \beta}{M_{H^\pm}^2} \kappa \left(\frac{m_l^2}{m_\tau^2}\right) \right], \quad (13)$$

where

$$\kappa(x) = \frac{g(x)}{f(x)}, \quad g(x) = 1 + 9x - 9x^2 - x^3 + 6x(1+x) \ln(x). \quad (14)$$

Note that the second term, coming from an interference with the SM amplitude, is much more important than the first one, that is suppressed by a factor $m_\tau^2 \tan^2 \beta / 8M_{H^\pm}^2$ that can be compensated only by a very large $\tan \beta$.

In 2HDM there are also one-loop contributions involving neutral as well as charged Higgs and Goldstone bosons. All these contributions are included in the G_F scheme as follows:

$$\begin{aligned} \Gamma_1^l &= \Gamma_0^l(1 + \delta Z_{L\tau} + \delta Z_{Ll} + \delta Z_{L\nu\tau} + \delta Z_{L\nu l}) + \Gamma_{loops}^{W^\pm} \\ &\quad + \Gamma_{tree}^{H^\pm} + \Gamma_{loops}^{H^\pm} + \Gamma_{CT}^{H^\pm}, \end{aligned} \quad (15)$$

where the first term corresponds to the SM prediction, $Z_{Lf} = 1 + \delta Z_{Lf}$ are the renormalisation constants for the left component of the fermion f and $\Gamma_{loops}^{W^\pm}$ corresponds to the one-loop corrections to the W^\pm exchange tree-level amplitude. The H^\pm exchange tree level contribution and its one-loop and counterterm corrections are described by $\Gamma_{tree}^{H^\pm}$, $\Gamma_{loops}^{H^\pm}$ and $\Gamma_{CT}^{H^\pm}$, respectively.

The H^\pm contribution is numerically small and the radiative corrections to this amplitude will be neglected here. Taking this into account we will just consider the tree-level expression eq.(13), implying that

$$\Gamma_{loops}^{H^\pm} = \Gamma_{CT}^{H^\pm} = 0. \quad (16)$$

5 One-loop 2HDM(II) corrections

We evaluate, in the 't Hooft-Feynman's gauge, the one-loop contributions coming from a 2HDM(II) to the quantities Δ^l , using definitions and conventions for one-loop integrals of [20]. In this computation, we will take into account the fact that the charged Higgs and W^\pm masses are very large compared with the leptonic masses and external momenta, and we will neglect masses of muon and electron in the loop calculation. This means that the obtained loop corrections are universal, i.e. they do not depend whether decay into e or μ is considered, so $\Delta_{oneloop}^\mu = \Delta_{oneloop}^e = \Delta_{oneloop}$. Moreover, we will focus on large $\tan\beta$ enhanced contributions involving the Yukawa couplings of the charged leptons.

5.1 Renormalisation constants

In order to evaluate the 2HDM contribution to the fermion fields renormalisation constants, one has to compute the self-energies coming from the diagrams shown in Fig. 4.

Charged lepton self-energies. There are two kinds of contributions, involving the exchange of a neutral and charged boson, respectively. The second ones are numerically negligible since they are proportional to m_l^2/M_W^2 and $m_l^2/M_{H^\pm}^2$ (for $\chi^+ = G^+$ and H^+ , respectively). Therefore we will consider the corrections coming from neutral Higgs and Goldstone bosons only. Since these corrections are proportional to m_l^2 we will take into account just the contributions to the τ self-energy. We obtain

$$\delta Z_{Le} = \delta Z_{L\mu} = 0$$

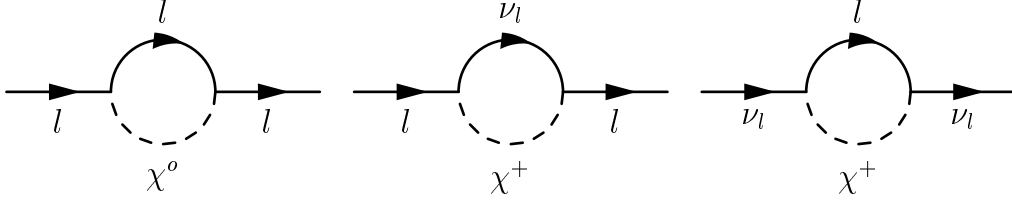


Figure 4: *Two-point diagrams contributing to the fermion fields renormalisation. Here $\chi^o = h, H, A, G^o$ and $\chi^+ = H^+, G^+$.*

$$\begin{aligned}
\delta Z_{L\tau} &= \Delta_\tau^h + \Delta_\tau^A + \Delta_\tau^h + \Delta_\tau^{G^o} \\
\Delta_\tau^h &= -\frac{G_F m_\tau^2 \sin^2 \alpha}{8\sqrt{2}\pi^2 \cos^2 \beta} \mathcal{B}(m_\tau^2; M_h^2, m_\tau^2) \\
\Delta_\tau^A &= -\frac{G_F m_\tau^2}{8\sqrt{2}\pi^2} \tan^2 \beta \mathcal{B}(m_\tau^2; M_A^2, m_\tau^2) \\
\Delta_\tau^h &= -\frac{G_F m_\tau^2 \cos^2 \alpha}{8\sqrt{2}\pi^2 \cos^2 \beta} \mathcal{B}(m_\tau^2; M_H^2, m_\tau^2) \\
\Delta_\tau^{G^o} &= -\frac{G_F m_\tau^2}{8\sqrt{2}\pi^2} \mathcal{B}(m_\tau^2; M_Z^2, m_\tau^2) \simeq 0.
\end{aligned} \tag{17}$$

where we use the following abbreviation

$$\mathcal{B}() = [B_0 + B_1 + 4m_\tau^2 B'_0 + 2m_\tau^2 B'_1]().$$

The G^o contribution will be neglected since it is not $\tan^2 \beta^2$ enhanced.

Neutrino self-energies. In this case only the H^+ and G^+ contributions are involved and, since again these corrections are proportional to the mass of the lepton in the loop, we will just consider the corrections to the tauonic neutrino field renormalisation. We obtain

$$\begin{aligned}
\delta Z_{L\nu_e} &= \delta Z_{L\nu_\mu} = 0 \\
\delta Z_{L\nu_\tau} &= \Delta_{\nu_\tau}^{H^+} + \Delta_{\nu_\tau}^{G^+} \\
\Delta_{\nu_\tau}^{H^+} &= -\frac{G_F m_\tau^2}{4\sqrt{2}\pi^2} \tan^2 \beta [B_0 + B_1](0; M_{H^\pm}^2, m_\tau^2). \\
\Delta_{\nu_\tau}^{G^+} &= \frac{G_F m_\tau^2}{4\sqrt{2}\pi^2} [B_0 + B_1](0; M_W^2, m_\tau^2) \simeq 0.
\end{aligned} \tag{18}$$

5.2 One-loop three-point contribution

The one-loop three-point diagrams contributing to Δ in the 2HDM(II) are presented in Fig. 5. We use here the following notations: $\chi^0 = h, H, A, G^o$, $\chi^+ = H^+, G^+$ and $(V, \phi) = (G^+, Z), (W^+, h), (W^+, H)/(Z, G^+)$

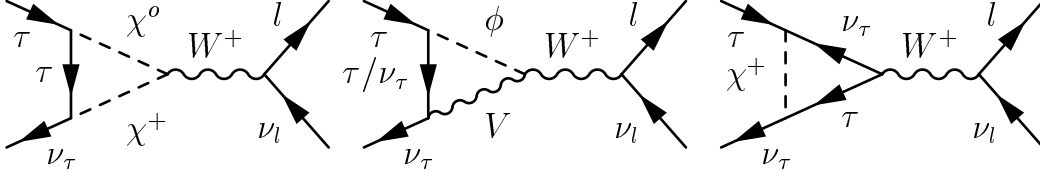


Figure 5: *Three-point diagrams contributing to the $W^\pm\tau\nu_\tau$ vertex correction. Similar diagrams exist for the $W^\pm l\nu_l$ vertex. $\chi^0 = h, H, A, G^o$, $\chi^+ = H^+, G^+$ and $(V, \phi) = (G^+, Z), (W^+, h), (W^+, h)/(Z, G^+)$.*

These $W^\pm l\nu_l$ vertex corrections are proportional to the lepton mass and therefore we will consider only the radiative contributions to the $W^\pm\tau\nu_\tau$ vertex. The different contributions coming from each diagram are as follows.

$\chi^+ - \chi^0 - \tau$ Loops. We have computed them (Fig. 5 left) in the limit of large M_{H^\pm} and M_W , this is, we have obtained the complete expressions and keep only such terms that do not decouple in the limit $M_{H^\pm}, M_W \gg m_\tau$. The resulting expressions are:

$$\begin{aligned}
\Delta_{loops}^{H+h} &= \frac{G_F m_\tau^2}{2\sqrt{2}\pi^2} \tan\beta \frac{\sin\alpha}{\cos\beta} \cos(\alpha - \beta) C_{20}(m_\tau^2, m_{\nu_\tau}^2; M_h^2, m_\tau^2, M_{H^\pm}^2) + \dots \\
\Delta_{loops}^{H+A} &= \frac{G_F m_\tau^2}{2\sqrt{2}\pi^2} \tan^2\beta C_{20}(m_\tau^2, m_{\nu_\tau}^2; M_A^2, m_\tau^2, M_{H^\pm}^2) + \dots \\
\Delta_{loops}^{H+H} &= -\frac{G_F m_\tau^2}{2\sqrt{2}\pi^2} \tan\beta \frac{\cos\alpha}{\cos\beta} \sin(\alpha - \beta) C_{20}(m_\tau^2, m_{\nu_\tau}^2; M_H^2, m_\tau^2, M_{H^\pm}^2) + \dots \\
\Delta_{loops}^{G+h} &= -\frac{G_F m_\tau^2}{2\sqrt{2}\pi^2} \frac{\sin\alpha}{\cos\beta} \sin(\alpha - \beta) C_{20}(m_\tau^2, m_{\nu_\tau}^2; M_h^2, m_\tau^2, M_W^2) + \dots \simeq 0 \\
\Delta_{loops}^{G+H} &= -\frac{G_F m_\tau^2}{2\sqrt{2}\pi^2} \frac{\cos\alpha}{\cos\beta} \cos(\alpha - \beta) C_{20}(m_\tau^2, m_{\nu_\tau}^2; M_H^2, m_\tau^2, M_W^2) + \dots \simeq 0 \\
\Delta_{loops}^{G+G^o} &= -\frac{G_F m_\tau^2}{2\sqrt{2}\pi^2} C_{20}(m_\tau^2, m_{\nu_\tau}^2; M_Z^2, m_\tau^2, M_W^2) + \dots \simeq 0
\end{aligned} \tag{19}$$

The three last contributions can be neglected in the large $\tan\beta$ limit.

$V - \phi - l$ Loops. These contributions (Fig. 5, middle) are numerically negligible as do not contain any $\tan^2\beta$ factor. Therefore, in our work

$$\Delta_{loops}^{V\phi} \simeq 0. \tag{20}$$

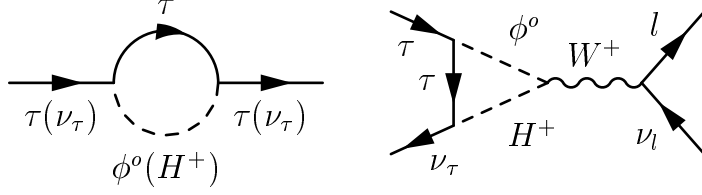


Figure 6: *Dominant one-loop diagrams contributing to leptonic τ decays in the limit of large $\tan\beta$, here $\phi^o = h, H, A$.*

$\tau - \nu_\tau - \chi^+$ Loops. We have computed these contributions (Fig. 5, right) and checked that they decouple in the limit of very heavy charged Higgs boson and W^\pm boson, as their leading terms in this limit are proportional to $\frac{m_\tau^2}{M_{H^\pm}^2}$ or $\frac{m_\tau^2}{M_W^2}$. Therefore

$$\Delta_{loops}^{\nu_l \chi^+} \simeq 0. \quad (21)$$

5.3 One-loop box diagrams

The one-loop box diagrams also contribute to the τ leptonic decays, all of them involving the exchange of a charged Higgs boson or a W^\pm boson. They can be safely neglected due to the mass dimension of the D integrals that describe these diagrams, namely

$$D_0 \simeq \frac{1}{M^4}, \quad D_\mu \simeq \frac{1}{M^3}, \quad D_{\mu\nu} \simeq \frac{1}{M^2}, \quad D_{\mu\nu\rho} \simeq \frac{1}{M}, \quad D_{\mu\nu\rho\gamma} \simeq \mathcal{O}(M^0). \quad (22)$$

Since M_{H^\pm} and M_W are very large, as compared to m_τ , they will drive the mass dependence of the integrals, so $M = M_{H^\pm}, M_W$. Therefore only the terms proportional to $D_{\mu\nu\rho\gamma}$ do not decouple and give relevant contributions. However, in the considered case of τ decays there are no such contributions and we can neglect box diagrams altogether:

$$\Delta_{loops}^{box} \simeq 0 \quad (23)$$

5.4 Final expression for one-loop contribution

Taking all this into account, the dominant diagrams in the limit of large $\tan\beta$ are reduced to the ones drawn in Fig. 6 and the contributions coming from these diagrams are

$$\Delta_{oneloop} = \frac{G_F m_\tau^2}{8\sqrt{2}\pi^2} \tan^2\beta \times$$

$$\begin{aligned}
& [-\cos^2(\beta - \alpha)\mathcal{B}(m_\tau^2; M_h^2, m_\tau^2) \\
& -\mathcal{B}(m_\tau^2; M_A^2, m_\tau^2) \\
& -\sin^2(\beta - \alpha)\mathcal{B}(m_\tau^2; M_H^2, m_\tau^2) \\
& -2[B_0 + B_1](0; M_{H^\pm}^2, m_\tau^2) \\
& +4\cos^2(\beta - \alpha)C_{20}(m_\tau^2, m_{\nu_\tau}^2; M_h^2, m_\tau^2, M_{H^\pm}^2) \\
& +4C_{20}(m_\tau^2, m_{\nu_\tau}^2; M_A^2, m_\tau^2, M_{H^\pm}^2) \\
& +4\sin^2(\beta - \alpha)C_{20}(m_\tau^2, m_{\nu_\tau}^2; M_H^2, m_\tau^2, M_{H^\pm}^2)]. \quad (24)
\end{aligned}$$

An easy to handle expression can be obtained from eq.(24) for neutral Higgs masses larger than the τ mass, $M_{\phi^0} \geq m_\tau$. Notice that no assumption on the Higgs spectrum is considered⁵. In this limit, we get

$$\begin{aligned}
\Delta_{oneloop} &\approx \frac{G_F m_\tau^2}{8\sqrt{2}\pi^2} \tan^2 \beta \tilde{\Delta} \\
\tilde{\Delta} &= \left[-\left(\ln \left(\frac{M_{H^\pm}^2}{m_\tau^2} \right) + F(R_{H^\pm}) \right) \right. \\
&\quad + \frac{1}{2} \left(\ln \left(\frac{M_A^2}{m_\tau^2} \right) + F(R_A) \right) \\
&\quad + \frac{1}{2} \cos^2(\beta - \alpha) \left(\ln \left(\frac{M_h^2}{m_\tau^2} \right) + F(R_h) \right) \\
&\quad \left. + \frac{1}{2} \sin^2(\beta - \alpha) \left(\ln \left(\frac{M_H^2}{m_\tau^2} \right) + F(R_H) \right) \right] \quad (25)
\end{aligned}$$

where $R_\phi \equiv M_\phi/M_{H^\pm}$ and

$$F(R) = -1 + 2 \frac{R^2 \ln R^2}{1 - R^2}. \quad (26)$$

Some useful limits of the F function are:

$$F(R \ll 1) \sim -1, \quad F(R = 1) = -3, \quad F(R \gg 1) \sim -(1 + 2\ln R^2). \quad (27)$$

In the following we will use the expressions (24) and (25) to explore the phenomenological consequences of the large $\tan \beta$ enhanced 2HDM(II) radiative corrections to the leptonic τ decays. A comparison of results obtained using the exact and approximated formulae will be given below.

5.5 Results for some interesting scenarios

In some phenomenologically interesting scenarios, the expression (25) can be simplified. In the case of light h and $\sin^2(\beta - \alpha) = 0$, Δ does not depend

⁵ We generalised here the result in [8] where assumptions were made $M_{H^\pm}, M_A \gg M_h$ and $\alpha = \beta$.

on M_H and two different assumptions can be made, $M_A = M_{H^\pm}$ and $M_A \ll M_{H^\pm}$, giving,

$$\tilde{\Delta} = \ln \frac{M_h}{M_{H^\pm}} + 1 \quad \text{and} \quad \tilde{\Delta} = \ln \frac{M_h}{M_{H^\pm}} + \ln \frac{M_A}{M_{H^\pm}} + 2, \quad (28)$$

respectively. Notice that when LEP is less sensitive to the h , because it does not couple to gauge bosons, $\tilde{\Delta}$ still depends logarithmically on its mass.

If A is light and $\sin^2(\beta - \alpha) = 1$, one obtains the same expression for Δ that in the previous case but replacing $h \rightarrow A$ and $A \rightarrow H$. Therefore any analysis with h light and $\sin^2(\beta - \alpha) = 0$ can be easily extended to the case of light A on $\sin^2(\beta - \alpha) = 1$.

In a SM-like scenario, with light h , $\sin^2(\beta - \alpha) = 1$ and very heavy, degenerate additional Higgs bosons, $\tilde{\Delta}$ is zero, showing clear decoupling. Note that this follows from the expression below, which hold for arbitrary $\sin(\beta - \alpha)$ and degenerate H, A, H^\pm case:

$$\tilde{\Delta} = \cos^2(\beta - \alpha) \left[\ln \frac{M_h}{M} + 1 \right]. \quad (29)$$

6 Numerical analysis

In this section we analyse the dependence of the 2HDM(II) corrections described in previous sections for the leptonic τ decays on the different Higgs boson masses and mixing angles. First we stress that the one-loop contribution dominates the 2HDM(II) effects, being for Δ^e five orders of magnitude larger than the tree-level H^\pm contribution in the interesting region of parameter space, and one or two orders of magnitude larger for Δ^μ . Therefore, although we will include the whole contribution in the numerical analysis, the main features of the 2HDM effects are described by the one-loop correction in eq.(25). In the following only results for muon decay channel will be presented. However we stress that the obtained one-loop corrections are the same for both electron and muon channels.

As all results are proportional to $\tan \beta^2$, they will be plotted for $\tan \beta = 1$, to be rescaled by $\tan \beta^2$.

In eq.(25) there are two contributions, one coming from the charged Higgs alone and the other one involving also the neutral Higgs bosons. The former is always negative and it becomes more negative for larger charged Higgs mass. The latter is always positive and it grows with the neutral Higgs masses. In this way the total 2HDM(II) radiative effects are the sum of two contributions of the same order and with different signs and therefore large corrections will appear when one of these contributions is dominating. Since the modulus of both corrections grow with the Higgs masses one expects large radiative effects in two cases: (i) heavy H^\pm and light ϕ^o (large negative corrections) and (ii) light H^\pm and heavy ϕ^o (large positive corrections). Taking into account the lower bound for M_{H^\pm} coming from $b \rightarrow s\gamma$, M_H^\pm above 490 GeV,

one expects to get large radiative effects in case (i) only. Note that in this (i) case the $\tilde{\Delta}$ (loop contribution) is negative, as well as the tree-level H^\pm exchange, eq.(13).

We will consider two scenarios of a special phenomenological interest: light scalar h and light pseudoscalar A .

6.1 Light scalar boson, h

Here we will consider a scenario with light scalar boson, h , M_h below 114 GeV, and degenerate heavy Higgs bosons, with masses $M_A = M_H = M_{H^\pm} = M$, above 300 GeV. For such a light Higgs boson h , its couplings to gauge bosons are constrained by LEP data as described in Fig. 1 (left), lying between 0 and $\sin(\beta - \alpha)^2|_{max}$. Note that for arbitrary $\sin(\beta - \alpha)$ and degenerate H, A, H^\pm we have eq.(29).

In this light h scenario and instead of degenerate additional Higgs bosons, one can also consider a case with SM-like Higgs boson H with couplings to the gauge bosons as for the SM Higgs, namely $\chi_V^H = 1$ (corresponding to $\sin(\beta - \alpha) = 0$). It is reasonable to assume that it has a mass in the region expected for a SM Higgs boson, say $M_H = 115$ GeV, although as follows from eq. (25) nothing depends on this mass. Contrary one gets here a clear dependence on mass of h ,

$$\tilde{\Delta} = \ln \frac{M_h}{M} + 1. \quad (30)$$

The different contributions to Δ are plotted in Fig. 7 (left) for $M_h = 5$ and 70 GeV. The total results are plotted using solid lines, while the one-loop contributions using dashed lines, respectively. As can be seen, the H^\pm tree-level effect is important for low M but the one-loop radiative contribution becomes dominant for $M \geq 500$ GeV. In particular the logarithmic dependence on M coming from the one-loop corrections is clearly seen. Notice that curves are plotted for $\sin^2(\beta - \alpha) = 0$ and $\sin(\beta - \alpha)^2|_{max}$, the maximum value allowed by LEP data. For h mass equal to 5 GeV the results for $\sin^2(\beta - \alpha)$ between 0 and 0.02 can not be distinguished.

The dependence of Δ on the light Higgs mass can be seen by comparing the results for $M_h = 5$ and 70 GeV, and explicitly in Fig. 7 (right) where the contributions for $M_A = 100$ GeV, $M_{H^\pm} = 4$ TeV, $\sin(\beta - \alpha) = 0$ are plotted as a function of M_h . The 2HDM(II) loop corrections decrease logarithmically when increasing M_h as described by eq.(30), so the lighter h the larger the radiative corrections. One can see that Δ decrease linearly when increasing $\sin^2(\beta - \alpha)$, in agreement with eq.(29).

In the case with SM-like H we have $\sin^2(\beta - \alpha) = 0$, then Δ becomes insensitive to the value of M_H , see eq.(25), as discussed already and all results obtained above in the $\sin^2(\beta - \alpha) = 0$ case holds also here.

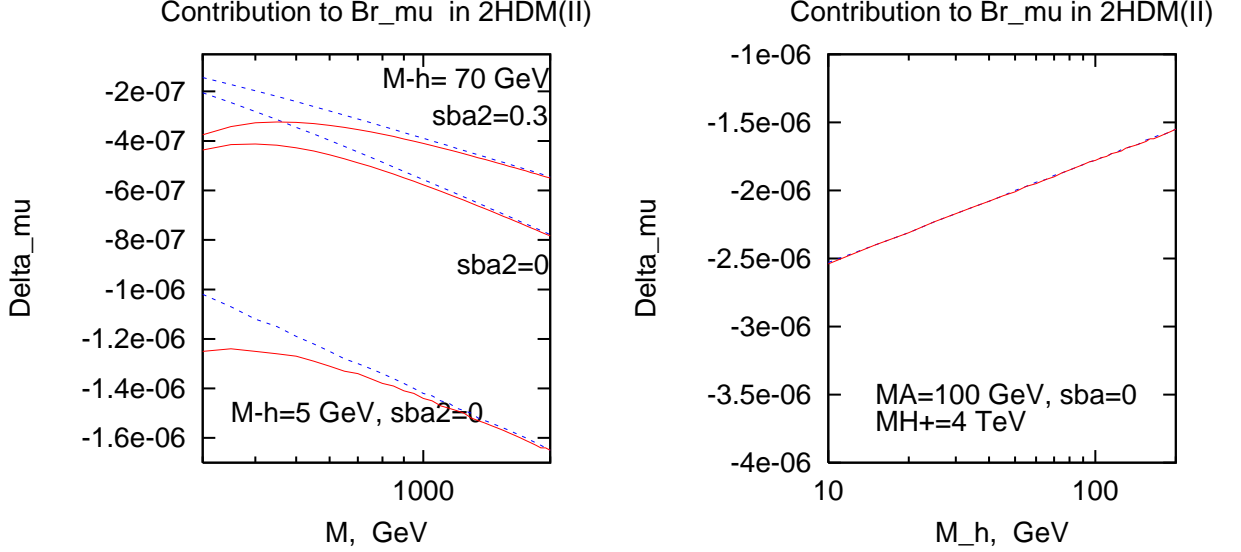


Figure 7: The total (solid line) and one-loop (dashed line) contributions to Δ for $\tan\beta = 1$ for $M_h = 5$ and 70 GeV, are plotted as a function of M . Results for mass of 70 GeV for $\sin^2(\beta - \alpha) = 0$ and 0.3 bottom and upper lines, respectively. Right: as a function of M_h for $M_A = 100$ GeV, $M_{H^\pm} = 4$ TeV and $\sin^2(\beta - \alpha) = 0$.

6.2 Light pseudoscalar, A

In the case where there is a light pseudoscalar, A , and $M_h = M_H$, the $\tilde{\Delta}$ does not depend on $\sin^2(\beta - \alpha)$. For $M_h = M_H = M_{H^\pm} = M$ we get

$$\tilde{\Delta} = \ln \frac{M_A}{M} + 1, \quad (31)$$

and it looks similar to the previous case of light h with $\sin^2(\beta - \alpha) = 0$ with obvious change M_h to M_A . Therefore we will not present the results corresponding to this case.

A light A scenario with an additional not very heavy h can also be studied. Here we choose the h mass to be equal to 100 GeV, that avoids direct conflict with LEP data as presented in Fig. 1 (left). In Fig. 8 the total contribution to Δ is plotted in solid lines, while one-loop effects as dashed lines, respectively. Also in this case we can see that the one-loop radiative effects dominant for large M scale. The deviation from the SM prediction is larger for $\sin^2(\beta - \alpha) = 0$.

6.3 Comparison of exact and approximated results

Results coming from eq.(24) and from the approximation eq.(25) have been plotted together in all the figures, being clearly indistinguishable. Therefore,

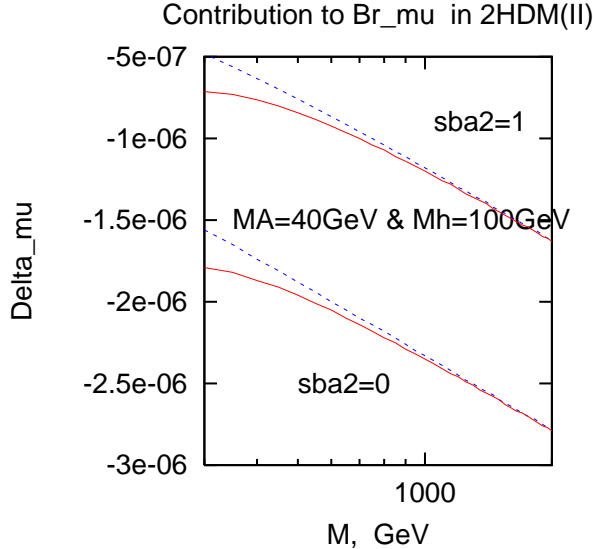


Figure 8: *The total (solid line) and one-loop (dashed line) contributions to Δ for $\tan\beta = 1$ for $M_A = 40$ GeV and $M_h = 100$ GeV for $\sin^2(\beta - \alpha) = 0$ and 1, bottom and upper lines, respectively.*

the easy formula eq.(25) can be used to describe the 2HDM(II) radiative corrections to the τ leptonic decays in the whole considered range of parameters.

7 Constraining 2HDM(II) by the τ data

In this section the constraints on 2HDM(II) parameters from the leptonic τ decay data will be obtained. The complementarity between LEP processes used for direct searches of light Higgs bosons and indirect searches through leptonic τ decays will be exploited to explore “pessimistic” scenarios for direct searches. In particular the case $\sin^2(\beta - \alpha) = 0$ will be studied since in this scenario Higgsstrahlung and VV fusion processes for h are suppressed. Experimental limits on Δ derived by us in Sect. 3 allow to set upper bounds on $\tan\beta$ for light M_h or M_A scenarios. We provide also exclusion for (M_h, M_A) plane for various $\tan\beta$ and $\sin(\beta - \alpha)$.

We also obtain new lower and upper bounds on the charged Higgs mass as a function of $\tan\beta$ from τ decays.

7.1 Bounds on the Yukawa couplings of the lightest neutral Higgs bosons

The upper limits on $\tan\beta$ (Yukawa coupling) for light M_h and light M_A scenarios are shown in Fig. 9, and 10, respectively.

In the “pessimistic” scenario of $\sin^2(\beta - \alpha) = 0$, leptonic τ decay data

can be exploited to set upper limits on couplings as a function of M_h , that one can compare with limits coming from other processes.

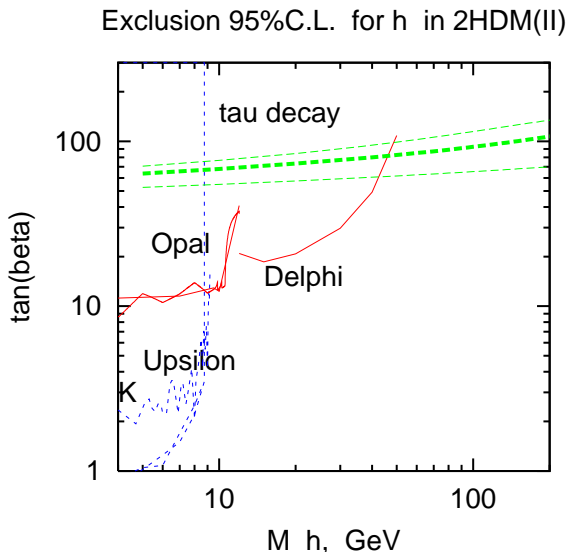


Figure 9: 95 %CL exclusion from τ decay for large $\tan\beta$ as a function of M_h compared to the existing limits from Yukawa processes at LEP and Upsilon decay. Two almost horizontal lines (in green) corresponds to $M_A = 100$ GeV and $M_{H^\pm} = 500$ GeV and 4 TeV, upper and lower lines, respectively. The results for degenerated A and H^+ with mass 4 TeV are plotted in thicker line.

In Fig. 9 the constraints on the Yukawa couplings set by leptonic τ decay data for h and $\sin(\beta - \alpha) = 0$ are drawn. One can see that these data provide upper limits on $\tan\beta$ in region inaccessible by other experiments, for mass above 45 GeV.

As a opposite case with a light Higgs boson one can consider the case with light pseudoscalar A . In the same scenario of $\sin^2(\beta - \alpha) = 0$, M_A can be low if the scalar h is heavy enough to suppressed associated production and it will be constrained just by data from the Yukawa process with $f\bar{f}A$ final state. Also in this case, leptonic τ decays can be used to set bounds on the Yukawa coupling as a function of M_A , see Fig. 10. The right panel shows the region around mass of A equal 10 GeV.

Since this scenario can be relevant in explaining $(g - 2)_\mu$ data, we plot in Fig. 11 the upper limits for $\tan\beta$ from τ decay and the allowed region from the newest $g - 2$ for muon data, in comparison all other existing limits. Degenerate masses of h, H, H^+ were assumed equal to 1 and 4 TeV, upper and lower lines respectively.

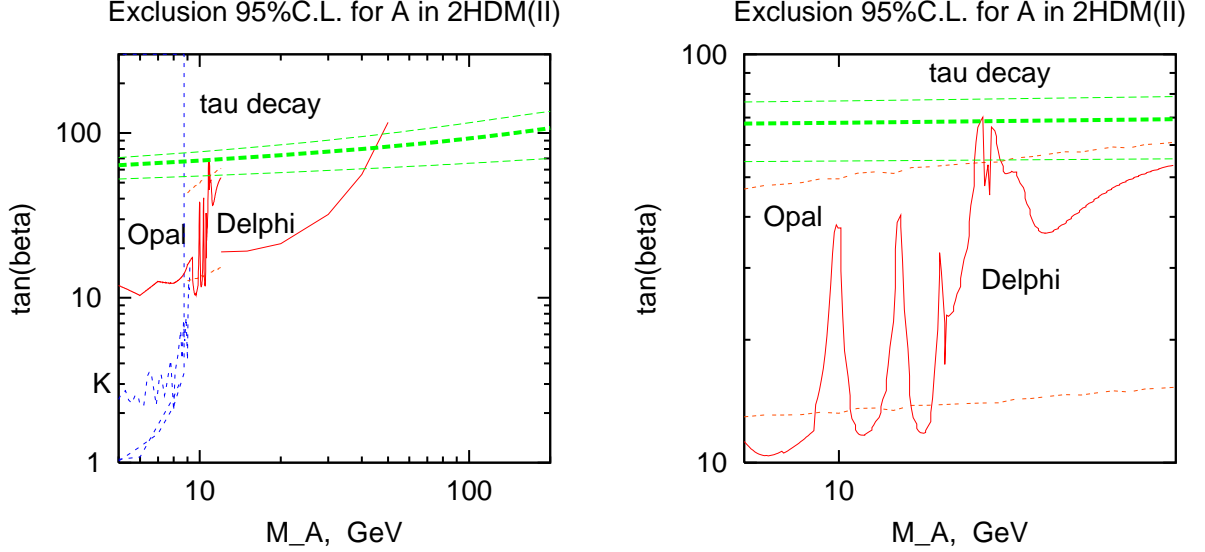


Figure 10: 95 %CL exclusion from τ decay for large $\tan\beta$ as a function of M_A compared to the existing limits from Yukawa processes at LEP and Upsilon decay. Two almost horizontal lines (in green) corresponds to $M_h = 100$ GeV and $M_{H^\pm} = 500$ GeV and 4 TeV, upper and lower lines, respectively. The results for degenerated h and H^\pm with mass 4 TeV are plotted in thicker line. Left: Mass range from 5 to 200 GeV, Right: mass range from 8 to 12 GeV.

7.2 Constraints on a low M_A & M_h scenario

An scenario with both light h and A will be also of phenomenological interest. Since Δ can be large for low M_h and M_A , the leptonic τ decay data can be used to set constrains in this scenario in the $M_h - M_A$ parameter space. The comparison of these constraints with the ones coming from direct searches will reveal the importance of indirect searches in τ decays.

In Fig. 12, the constrained regions in the $M_h - M_A$ plane for $\sin^2(\beta - \alpha) = 0$ are showed, to be compared to Fig. 1 (right). These regions, symmetric in M_h and M_A , constrain the possibility of both h and A being very light. For large values of M_{H^\pm} and $\tan\beta$ the 2HDM(II) effects can be very large and some of the regions of the parameter space allowed by direct searches can be forbidden by indirect effects on τ data. In order to show this point, the line $M_h + M_A = 130$ GeV has been plotted in Fig. 12 as an evaluation of the limit coming from LEP searches through associated production.

7.3 Constraints on the mass of charged Higgs boson

From the leptonic tau decays one can derive the limits on mass of charged Higgs boson as a function of $\tan\beta$. This is a standard source of limits for charged Higgs boson mass, what can be found in almost all papers devoted

Exclusion 95%C.L. for A in 2HDM(II)

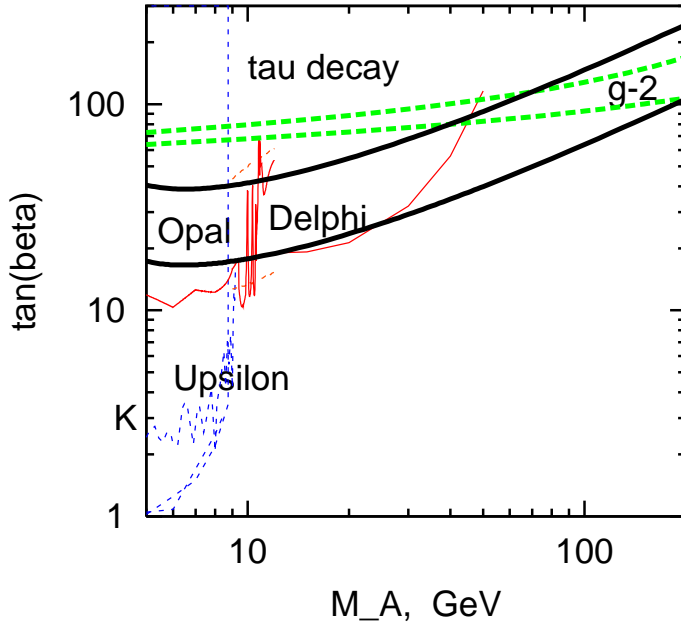


Figure 11: *Upper limits for $\tan\beta$ from τ decay and the allowed region from the newest $g - 2$ for muon data, in comparison all other existing limits. Degenerate masses of h, H, H^+ were assumed equal to 1 and 4 TeV, upper and lower lines respectively.*

to this subject - both theoretical and experimental ones. Such derivation is based on the tree level contribution for the muon channel, see eg [1].

If, as in all previous analysis, one uses only the tree-level contribution (for muon) then the following lower limit is obtained based on current Δ^μ value. Using the lowest value for 95% CL deviation from SM prediction (eq. 10) one gets

$$M_{H^\pm} \gtrsim 1.71 \tan\beta \text{ GeV}, \quad (32)$$

to be compared to the corresponding results from [21], [22], with a coefficient 1.86 and 1.4, respectively. This is nothing else, up to the lepton mass ratio, what issued as the Michel parameter η for the 2HDM (II).

However, we know that the loop effects are more important than the tree contribution, and one can not neglect them in the derivation of the constraints. Since $\Delta_{oneloop}$ grows with M_{H^\pm} , it allows to put upper bounds on M_{H^\pm} in scenarios with light neutral Higgs bosons. In particular, for $\sin^2(\beta - \alpha) = 0$, Δ goes as $\ln(M_{H^\pm}/M_h) + \ln(M_{H^\pm}/M_A)$ and therefore stronger upper bounds will be obtained for light h and A .

In Fig. 13 (left) the lower and upper bounds on M_{H^\pm} has been plotted as a function of $\tan\beta$, as obtained from the tree H^\pm exchange diagram only and from loop contribution only, respectively. The loop contribution are plotted

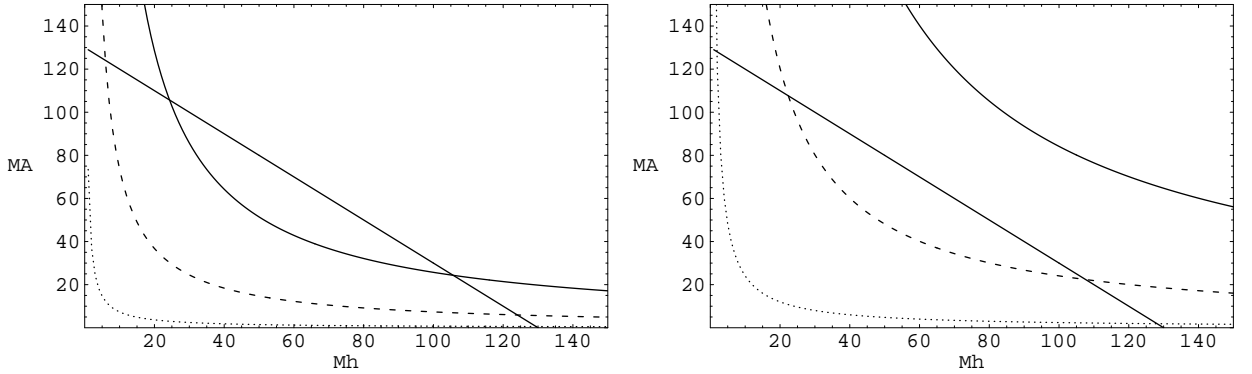


Figure 12: *Constrained regions in the $(M_h - M_A)$ plane for $\sin^2(\beta - \alpha) = 0$ and $\tan \beta = 60, 75, 90$ in dotted, dashed and solid lines respectively. $M_{H^\pm} = 500$ GeV on the right and 1 TeV on the left. $M_h + M_A = 130$ GeV plotted in solid line.*

for $\sin(\beta - \alpha) = 0$ and various mass of h , 5, 20 and 100 GeV, assuming degeneracy in masses of A and H^\pm . Upper limits coming from loop are plotted both for the muon and electron decay channels, the limits from electron one is slightly weaker (dashed (green) lines). The relevant limits from the tree H^\pm contribution is obtained only from muon channel, this is presented in the figure. The lower bound coming from $b \rightarrow s$ analysis is also shown for a comparison.

In Fig. 13 (right) we present full bounds coming from a sum of tree and loop contribution (thick lines) - giving a lower and upper limits for $M_h = 20$ GeV, $\sin(\beta - \alpha) = 0$. It is clear that the constraints for mass of H^+ changes drastically if the loop contribution is included in the analysis, and only if the SM-like scenario for h is considered, $\sin(\beta - \alpha) = 1$ and all other Higgs boson mass degenerate, tree contribution gives a reliable estimation.

Based on results presented in Fig. 14 the restrictions can be set on M_{H^\pm} for large values of $\tan \beta$ ($\tan \beta \geq 60$). In particular, in a scenario with light h and not so heavy A , M_{H^\pm} should be lower than 3 TeV for $\tan \beta = 65$. Although large values of $\tan \beta$ are required, this upper bound to the charged Higgs mass is important due to the difficulty on setting upper bounds on masses of undiscovered particles.

8 Conclusions and Summary

In this work we have computed the 2HDM(II) radiative corrections to the leptonic τ decays. As a first result we have obtained that these radiative effects are larger than the tree-level H^\pm contribution in the relevant regions of the parameter space. Our analysis has been focused on the $\tan \beta$ enhanced contributions and an easy-to-handle formula has been computed describing these one-loop effects in the approximation of Higgs masses larger than the

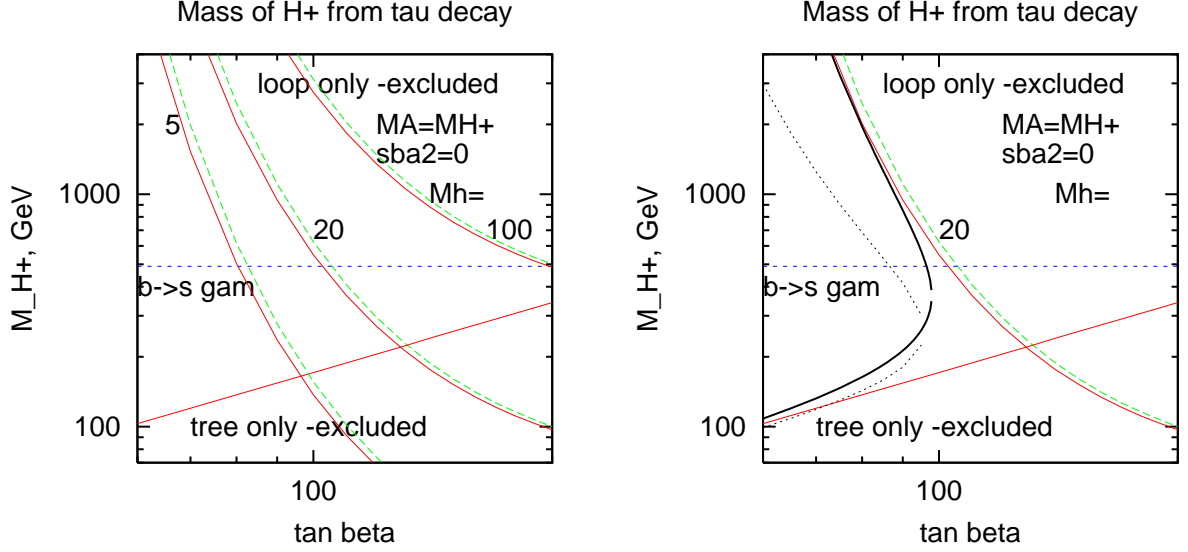


Figure 13: *Independent limits on mass of charged Higgs boson mass from one-loop (from electron (dashed line) and muon (solid line) channels) and tree H^+ exchange from muon channel. Left: Results from loop corrections for $M_h = 5, 20, 100$ GeV and $\sin^2(\beta - \alpha) = 0$, assuming $M_A = M_H^+$. The dashed lines corresponds to limits from Δ^e . Right: For $M_h = 20$ GeV the constraint from full (loop plus tree) contribution to Δ^μ , for degenerate $M_A = M_{H^\pm}$ (solid), and for $M_A = 100$ GeV (dotted) is plotted. Lower limit from $b \rightarrow s\gamma$ is also shown.*

τ mass. This formula allows us to study all the 2HDM parameter space in an intuitive way.

After the numerical analysis of the corrections, the constraints on the 2HDM(II) parameters from the leptonic τ decay data have been obtained in different scenarios. In particular the “pessimistic” scenarios for direct searches of light Higgs bosons at LEP have been intensively analysed. From this analysis we have obtained upper limits on the Yukawa couplings for both light h and light A scenarios, constraining also the low M_h & M_A scenario. We have derived new lower limits on M_{H^\pm} , different from the ones coming from tree-level effects, and we have also obtained interesting upper limits on M_{H^\pm} as a function of $\tan\beta$.

Therefore, from this analysis, one can conclude that leptonic τ decay data constrains 2HDM(II) scenarios with large $\tan\beta$, heavy H^\pm and light neutral Higgs bosons.

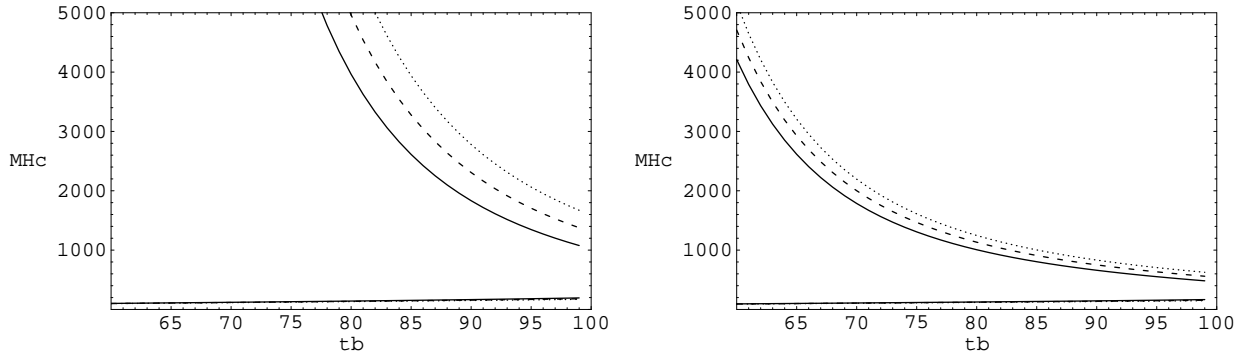


Figure 14: Limits on the $(M_{H^\pm} - \tan \beta)$ parameter space, in the light h scenario with $M_h = 40, 50, 60$ GeV (solid, dashed and dotted lines respectively) and $\sin^2(\beta - \alpha) = 0$. $M_A = M_{H^\pm}$ in the left panel while $M_A = 100$ GeV in the right one. Allowed regions are on the left of the curves.

9 Acknowledgement

The authors thank Theory Group at CERN for a kind hospitality allowing us to work on a final version of the paper and M. J. Herrero for fruitful discussions. MK is grateful for important discussions with Z. Wąs, B. Stugu and W. Marciano. This work was partially supported by the Polish Committee for Scientific Research, grant no. 1 P03B 040 26 and project no. 115/E-343/SPB/DESY/P-03/DWM517/2003-2005 and the European Community's Human Potential Programme under contract HPRN-CT-2000-00149.

References

- [1] S. Eidelman et al., Phys. Lett. **B592**, 1 (2004)
- [2] J.F. Gunion, H.E. Haber, G.L. Kane and S. Dawson, *The Higgs Hunter's Guide*, Addison-Wesley Publishing Company, Reading, MA, 1990. J. F. Gunion and H. E. Haber, Phys. Rev. D **67** (2003) 075019 [arXiv:hep-ph/0207010].
- [3] The DELPHI Collaboration. DELPHI 2002-037-CONF-571. G. Abbiendi *et al.* [OPAL Collaboration], Eur. Phys. J. C **23** (2002) 397 [arXiv:hep-ex/0111010].
- [4] P. Gambino and M. Misiak, Nucl. Phys. **B 611**, 338 (2001)
- [5] The OPAL Collaboration. OPAL PHYSICS NOTE PN509 (ICHEP 04). D. Horvath [OPAL Collaboration], Nucl. Phys. A **721** (2003) 453.
- [6] P. Chankowski, M. Krawczyk and J. Zochowski, Eur.Phys.J. **C 11**, 661 (1999).

- [7] K. Cheung and O.C.W. Kong, Phys. Rev. **D68** 053003 (2003).
- [8] W. Hollik and T. Sack, Phys. Lett. **B 284** 427 (1992)
- [9] A. Akeroyd, A. Arhrib, E. M. Naimi, Phys.Lett. **B490** 119 (2000) and references therein.
- [10] I. F. Ginzburg, M. Krawczyk and P. Osland, “Two-Higgs-doublet models with CP violation,” arXiv:hep-ph/0211371.
I. F. Ginzburg and M. Krawczyk, “Symmetries of two Higgs doublet model and CP violation,” arXiv:hep-ph/0408011.
- [11] I. F. Ginzburg, M. Krawczyk and P. Osland, arXiv:hep-ph/0101331. Nucl. Instrum. Meth. A **472** (2001) 149 [arXiv:hep-ph/0101229].
- [12] S. Kanemura, Y. Okada and E. Senaha, arXiv:hep-ph/0410048.
S. Kanemura, Y. Okada, E. Senaha and C. P. Yuan, arXiv:hep-ph/0408364.
S. Kanemura, S. Kiyoura, Y. Okada, E. Senaha and C. P. Yuan, Phys. Lett. B **558**, 157 (2003) [arXiv:hep-ph/0211308]. arXiv:hep-ph/0209326.
- [13] A. Arhrib, W. Hollik, S. Penaranda and M. Capdequi Peyranere, Phys. Lett. B **579**, 361 (2004).
- [14] G. W. Bennett *et al.* [Muon g-2 Collaboration], Phys. Rev. Lett. **92**, 161802 (2004) [arXiv:hep-ex/0401008],
H. Deng [Muon g-2 Collaboration], arXiv:hep-ex/0408148.
- [15] A. Hocker, arXiv:hep-ph/0410081.
S. I. Eidelman, Acta Phys. Polon. B **34** (2003) 4571.
A. Nyffeler, Acta Phys. Polon. B **34**, 5197 (2003).
- [16] M. Krawczyk, “Precision muon g-2 results and light Higgs bosons in the 2HDM(II),” Acta Phys. Polon. B **33** (2002) 2621 [arXiv:hep-ph/0208076].
- [17] The OPAL Collaboration: G. Abbiendi, et al. Phys. Lett. **B597** 11 (2004).
- [18] The OPAL Collaboration: G. Abbiendi, et al. CERN-PH-EP/2004-039 (hep-ex/0408097).
- [19] M. Neubert, Renormalization-Group Improved Calculation of the $B \rightarrow X_s \gamma$ Branching Ratio (hep-ph/0408179).
- [20] W. Hollik, in *Precision Tests of the Standard Electroweak Model*, edited by P. Langacker (World Scientific, Singapore, 1995), p. 37-116.
- [21] M.T. Dova, J. Swain and L. Taylor, Phys. Rev. **D58**, 015005 (1998).
- [22] A. Stahl and H. Voss, Z. Phys. **C74**, 73 (1997).